King Saud University

Journal of King Saud University – Science

www.ksu.edu.sa
www.sciencedirect.com

CrossMark

Characterisation of clay samples from minerals–rich deposits for thermoluminescence applications

Felix S. Olise [a,b,*], Solomon B. Ola [b], Fatai Akintunde Balogun [c]

[a] Department of Physics and Engineering Physics, Obafemi Awolowo University, Ile-Ife, Nigeria
[b] Department of Physics, University of Ibadan, Ibadan, Nigeria
[c] Centre for Energy Research and Development, Obafemi Awolowo University, Ile-Ife, Nigeria

Abstract Thermoluminescent (TL) characteristics of clay samples from Ijero-Ekiti and Isan-Ekiti, Ekiti State, Nigeria were studied for application in retrospective dosimetry. In order to increase the potentials of the clay material for relevant radiation measurement applications, characteristic glow curves of samples from the clay deposits have been obtained using a Victoreen (2800M) TL reader and the TL properties subsequently examined. The variable heating rate method was used to determine the glow peak shape and intensity by estimating the activation energy or trap depth, E and the frequency factor, S. Most samples demonstrated the dependence of their glow curve on the heating rate, with the peak temperature, T_m increasing with the heating rate. These glow peaks were noted to be a complex trapping system, consisting of several overlapping first order peaks and each with different TL behaviour, except for certain samples, which showed independence of peak temperature with dose. While recommending further heating protocol to isolate each peak for the calculation of other kinetic parameters, we present an approximate 0.29–0.84 eV for E and 3.7×10^1 to $4.0 \times 10^6 \, \text{s}^{-1}$ for S. Though the samples with the TL dosimetric property of increased peak intensity with increasing excitation dose could be considered for TL applications, the reduction in TL intensity must be considered for high heating rates applications.

© 2017 The Authors. Production and hosting by Elsevier B.V. on behalf of King Saud University. This is an open access article under the CC BY-NC-ND license (http://creativecommons.org/licenses/by-nc-nd/4.0/).

1. Introduction

Radiation emergencies such as nuclear war, warhead tests, nuclear strikes by terrorists and radiological accidents pose potential threat to the safety and survival of man and his environment. In these events, routine monitoring is often insufficient to provide estimates of doses received by the radiation workers, the general public and the environment. In order to effectively monitor doses from these sources, retrospective dosimetry using luminescence methods becomes relevant.

ELSEVIER | **Production and hosting by Elsevier**

These methods are based on heated materials such as the various ceramic materials. Ceramic materials are mostly clay and often contain quartz and/or feldspar that serve as the active phosphor for measurement. Recently, studies have been carried out to identify and characterise adequate radiation sensitive materials, which can be used as emergency dosimeters (Woda et al., 2002). These materials could be those carried close to the human body or universally available.

Efforts have been made to separate and employ naturally occurring local materials for the development of thermoluminescence dosimeters (TLD) and other applications. In this regard, many materials or minerals such as quartz, feldspar, fluorspar, dolerite, marble and muscovite have been variously studied to determine their suitability for such applications (Balogun et al., 1999; Ogundare et al., 2004, 2005, 2006a; Ige et al., 2006; Fasasi et al., 2007; Egbe et al., 2010; Mokobia, 2010, 2012). A variety of materials such as cane sugar, egg shell and chalk have also been examined for their TL potentials (Iyang et al., 2011). Ige et al. (2006) studied the TL response of gamma-irradiated muscovite samples from two granite pegmatite deposits in Ilesha and Ijero-Ekiti, Nigeria. While using a heating rate of 8 °C/s, the authors showed that the glow curves and the TL sensitivity were deposit dependent. This was due to the TL peaks observed around 238 and 330 °C in one and only 238 °C in the other. Furthermore, the glow peaks demonstrated a super-linear response at low doses while the response was between linear and sub-linear for the high doses. Relatively, the TL signal remained stable judging from the fading studies carried out over a period of one month. The results showed that muscovite has a lot of potential as a phosphor material in retrospective dosimetry and TL dating applications. Egbe et al. (2010) investigated the basic thermoluminescence properties of clay sourced from Calabar, Cross River State, Nigeria. The samples were irradiated with x-rays in the diagnostic energy range. The results showed that the TL output of the samples was very low, but demonstrated enhanced performance with the addition of common salt (NaCl). The clay samples' water absorbing property offered a means of overcoming the hygroscopic nature of common salt at those diagnostic radiological doses.

More than 80 deposits of clay raw material are widely distributed in Nigeria (Aramide et al., 2014) and the most prominent type is the clay kaolin (Okunola and Egbulem, 2015). Mineral ores hosted by these deposits include but not limited to tantalite, tin and other precious stones; and this has resulted in mostly skeletal artisanal mining for their economic benefits. Given the abundance and the vast industrial potentials of the available clay deposits, the Nigerian clay has been largely underutilised. Most other known characterisations, especially from the famous Ijero-Ekiti and Isan-Ekiti deposits, are either for other industrial applications such as ceramic and refractories (Oyinloye and Adebayo, 2005; OlaOlorun and Oyinloye, 2010; Ologe et al., 2014; Akinola et al., 2014) or background radiation level measurements (Olise et al., 2016). In order to widen the industrial potentials of these deposits, there is the need to further characterise the clay samples, especially from the deposits with minerals similar to those already studied.

Thus, this study is aimed at investigating the potential of the clay samples from the Ijero-Ekiti and Isan-Ekiti deposits for application in retrospective dosimetry. The features of clay specimens as good candidates for such dosimeters include increase in intensity peak with gamma excitation dose (McKeever, 1985). This study also investigates the dependence of the TL on the heating rates and the other glow curve factors.

2. Materials and methods

2.1. Description of the study areas

The study areas considered are located in Ijero-Ekiti and Isan-Ekiti, both in Ekiti State, South-western Nigeria. Ekiti State is entirely underlain by crystalline basement complex rocks of the gneiss- schist complex, the meta-sediments and meta-volcanic series and the Pan African granitoids–older granites (Malomo, 2011). These are composed of gneisses, schists, quartzite migmatite, charnockite, diorites, granites, granodiorites and pegmatites. The older granites are of the Precambrian-Cambrian age (Malomo, 2011).

Ijero-Ekiti plays host to a number of important minerals such as cassiterite and tin ore, columbite and foundry sand. Due to the available minerals in these deposits, Ijero area is characterised by frequent and different kinds of mining operations. The two deposits considered in Ijero are the Oke-asa and Oke-kusa deposits, both located on the hills. From the field observations, the deposits were characterised by well-dug mining pits. Oke-asa is known for its characteristic white colour clay. The minerals mined at Oke-asa include feldspar, marble and charnockite. The Oke-kusa clay deposit plays host to minerals such as kaolin, gemstones, mica, cassiterite and quartz.

Isan Ekiti in Oye local government area is considered a residual and partially reworked kaolin deposit varying from 10 to 20 m thick, with up to 1 m of overburden, overlying weathered gneiss and charnockite intruded by pegmatite (Malomo, 2011). Ceramic (ball) and kaolinite clays available in these deposits are used as raw material for abrasive, plastics, ceramic wares, pharmaceuticals, textiles, fertilizers, white tiles, insulator wares and pencils (Malomo, 2011).

2.2. Sample collection and preparation

Sample collection was conducted in February, 2015 during the dry season. In all, 13 samples, each weighing about 500 g was collected from the three different clay deposits using the standard geological techniques (Akinola et al., 2014) and the point sampling method. At all the sampling points, the exposed surface of the excavated clay was removed of overlaying organic matter using a hand trowel. The samples, which appeared in clustered form, were collected and sealed in separate polyethylene bags to prevent cross contamination. In Ijero, six (6) and two (2) samples were collected from Oke-kusa and Oke-asa deposits, respectively while five (5) samples were collected at Isan. The Oke-kusa samples presented white, grey and brownish-red colouration while those from Oke-asa presented a greyish, almost white colouration. The Isan samples were dark-grey, reddish-brown to off-white in colour. These suggest the presence of minerals such as Iron and Calcium.

The as-received samples were air-dried to achieve constant weights and subsequently pulverised using agate mortar and pestle. This was to facilitate the sieving process with a grain size of less than 200 μm. The sample preparation procedure was carried out at room temperature. In order to empty the trap sites of the stored energy due to natural radiation, the

samples were annealed. The annealing was carried out using an industrial oven at the Department of Geology, University of Ibadan, Nigeria at a temperature of 400 °C for two hours. This choice was made since it was sufficient to erase the effect of previous irradiation (Ige et al., 2006; Kaur et al., 2013); and to prevent excessive crystal rearrangement or damage which may occur at higher temperatures annealing. Also, the TLD reader's maximum operational temperature is 400 °C. To prevent crystal damage from the higher temperature annealing (Ige et al., 2006), each sample was thereafter allowed to cool rapidly at room temperature. Two portions of each sample of about 1.5 g, were weighed out and wrapped into black polyethylene sachets. They were then kept in a desiccator prior to irradiation. The thinly spread-out samples had about 2 mm wall thickness.

2.3. Sample irradiation and thermoluminescence (TL) measurement

The samples were irradiated using a Canadian Atomic Energy made ^{60}Co gamma source (Gammabeam X200). The facility was accessed at the Secondary Standard Dosimetry Laboratory (SSDL) of the National Institute of Radiation Protection and Research (NIRPR), University of Ibadan, Nigeria. The irradiations were carried out at room temperature, pressure and humidity, with the source dose rate of 65.33 Gy/h at the irradiation point of 80 cm from the source. The test dose of about 5 and 10 Gy were delivered to each sample placed at 80 cm from the source.

The TL measurements were carried out using a Victoreen TL reader (Model 2800 M). The TL reader at the Centre for Energy Research and Development (CERD), Obafemi Awolowo University, Ile-Ife, Nigeria has a heating rate range of between 5 and 30 °C/s. The readouts were obtained from about 20 mg of these samples, which were carefully placed and thinly spread-out on the planchet to avoid accidental spill and ensure good thermal contact, respectively. For all the measurements, a pre-heat temperature of 50 °C was employed for 10 s in order to eliminate glow peaks due to low temperatures. For each sample run, two measurements were made; one after the other and each from 50 °C. In each case, the second measurement data were subtracted from the first in order to correct for the effect of blackbody radiation from the sample holder (Ogundare et al., 2006b). After the read cycle was completed, the chamber was left closed until the planchet temperature had fallen below 50 °C. This step was repeated with the sample drawer and planchet thoroughly cleaned of sample left overs before the next sample run. The PC coupled to the reader displayed the results. The readout was carried out in a dark TLD room but with a 25 W red bulb, providing minimal illumination in order to prevent exposure to ultraviolet radiation.

2.4. Kinetic parameters characterisation

A set of parameters characterise the shape and intensity of a glow peak. These are the activation energy, E; the frequency factor, S; the number of electrons, n_o trapped in the defect centres at the start of the heating; and the order of kinetics, b (Ogundare and Chithambo, 2006). The methods for the analysis of the glow curve for the said parameters include those based on the use of the peak shape; the heating rate; and the

computerised deconvolution of the glow curve. In this work, the variable heating rate method (VHR) was adopted (Yazici et al., 2002; Ogundare and Chithambo, 2006).

The increase in glow-peak temperature, T_m of a given glow peak with the heating rate, β is employed in the VHR method for calculating the activation energy (Hoogenstraaten, 1958; Ogundare and Chithambo, 2007). For the discrete values of the activation energy, a plot of $\ln (T_m^2/\beta)$ against $1/T_m$ should give a straight line with the gradient, E/k and intercept, $\ln(E/Sk)$; where k is the Boltzmann's constant and E is the kinetic parameters (Gökçe et al., 2009). The frequency factor, S can therefore be estimated from the gradient and the intercept (Gökçe et al., 2009).

3. Results and discussion

3.1. TL glow curves

For all the measurements, it was observed that the intensity at 5 °C/s heating rate was very low compared with those of the higher heating rates (10, 15 and 20 °C/s). At 5 °C/s heating rate, the maximum reader's temperature, for all the measurements, was about 250 °C. Hence, this heating rate could have been useful in evaluating the low-temperature peaks in the samples. However, due to the very low intensity of the curves, no peak was observed for all the samples. This is in agreement with the result of Ige et al. (2006) and further proves that the glow peaks could only be observed with heating rates greater than 8 °C/s and at doses lesser than 750 Gy. Therefore, we present maximum peak intensity, peak temperature and normalised peak intensity data for 10, 15 and 20 °C/s heating rates (Table 1) and only the glow curves obtained at 15 °C/s heating rate. Fig. 1a–m shows the glow curves of the samples irradiated to 5 and 10 Gy doses and read out at 15 °C/s. The effects of the increasing dose on the TL intensities and shapes of the curves for the various samples are depicted by the figures. The curves also indicate that the peak positions are affected by the increasing excitation dose.

While some samples present decreasing TL intensity with increasing dose at more than one peak temperatures and with dose-dependent glow curve shapes, others show fairly constant TL intensity for the doses with both curves presenting a peak at practically the same temperature. The broad peak observed for the higher dose curve suggests the presence of overlapping peaks (for example, Fig. 1a). This suggests closely spaced trapping centres for which individual glow peaks could not be resolved (Balogun et al., 1999). For such complex trapping system, a thermal cleaning procedure as described by Kirsh (1992) would be necessary to obtain the individual peaks. The fairly constant TL intensity at 5–10 Gy doses, for the second category of samples, could be due to trap saturation at doses above 5 Gy. Hence, for this range of doses, the stated peak would not be suitable for dosimetric applications as TL intensity should increase with dose. For the lower doses (such as 5 Gy), the glow curves (for example, Fig. 1b) could have peaks with intensities higher than those of the corresponding peaks (a broad peak with a shoulder) for the higher doses (10 Gy doses). The reduction in intensity at such two peaks also suggests the saturation of the peaks.

For both excitation doses, broad peaks stretching over about 50 °C were observed in some samples while in others,

Table 1 Variation of the observed peak intensity, I_m; glow-peak temperature, T_m and normalised peak intensity with the heating rate, β.

Sample	Maximum peak intensity, I_m (A.U)			Peak temperature, T_m (°C)			Normalised peak intensity		
	$\beta = 10$ °C/s	$\beta = 15$ °C/s	$\beta = 20$ °C/s	$\beta = 10$ °C/s	$\beta = 15$ °C/s	$\beta = 20$ °C/s	$\beta = 10$ °C/s	$\beta = 15$ °C/s	$\beta = 20$ °C/s
A	5.62E−08	3.37E−08	7.80E−08	314	328	340	5.63E−09	2.25E−09	3.90E−09
B	9.44E−09	1.01E−08	2.08E−08	267.5	293.36	310.75	9.44E−10	6.76E−10	1.04E−09
C	4.34E−09	8.27E−09	6.91E−09	310.77	329.63	345.25	4.34E−10	5.51E−10	3.46E−E−10
D	4.26E−08	5.09E−08	6.84E−08	296	324.95	350.25	4.26E−09	3.40E−09	3.42E−09
E	1.28E−07	1.49E−07	ARL	283.04	288.63	ARL	1.28E−08	9.94E−09	ARL
F	7.60E−08	5.94E−08	1.01E−07	272.75	292.68	309	7.60E−09	3.96E−09	5.05E−09
G	3.09E−07	3.04E−E−07	3.91E−07	250	267	280	3.09E−08	2.02E−08	1.95E−08
H	1.15E−08	2.17E−08	2.38E−08	338	331.97	373.75	1.15E−09	1.45E−09	1.19E−09
I	2.72E−08	2.96E−08	3.66E−08	290	318	338.75	2.72E−09	1.98E−09	1.83E−09
J	2.02E−7	1.09E−07	3.75E−07	314.75	328	338.75	2.02E−08	7.27E−09	1.87E−08
K	9.21E−08	1.12E−07	5.00E−08	310.25	329.63	345.25	9.21E−09	7.47E−09	2.50E−09
L	1.32E−09	2.21E−09	3.18E−09	194.75	268.79	169	1.32E−10	1.48E−10	1.59E−10
M	1.12E−08	2.12E−08	2.67E−08	319.25	332.63	342.25	1.12E−09	1.41E−09	1.34E−09

ARL – Above Reading Limit.

each curve consisted of two low and high-temperature peaks, indicating a minimum of two different charge traps in the samples (Fig. 1c, e, f & h). The low temperature peak presented constant intensity and shape for both doses while the high temperature peak had varying intensity, shape and temperature with dose. The variations in the curve patterns suggest that this category of samples would be unsuitable for dosimetric applications, especially for doses in the range of 5–10 Gy and particularly for the same heat treatment employed in this study.

Some samples have a single clear peak implying, at least, one high-temperature charge trap. The intensity of the curves decreases with increasing dose for some category and vice versa for others. However, the shape of the curve and peak temperature is independent of the excitation doses. This suggests that the high-temperature peak could be suitable for dosimetric applications for doses below 5 Gy for the earlier category of samples while the observation in the latter category is an indication that the peak is of the first order kinetics (Ige et al., 2006; Ogundare et al., 2006a). This kind of deep trap site, responsible for storing energy from radiation, is an important property when considering a material for dosimetric application. This is because such a trap site may indicate a high stability and low fading of TL signal. Low fading of signals implies that the high temperature heating needed to empty such trap is not readily obtainable from the environment. Although the TL output of this category of samples was low, the presentation of a single isolated peak also makes it worth considering for dosimetric applications. Also noted is a variation in the second category of samples, which demonstrated a clear dependence of the glow curve shape on the excitation dose. The observed single isolated peak shifted towards higher temperatures for higher excitation radiation doses (for example, Fig. 1k). If we assume that the peak is complex with several overlapping first-order glow peaks and each with different TL behaviour (Ogundare et al., 2006a), it can be explained that the glow peak is going through a maximum as the irradiation dose increases. The higher-temperature components of the complex peak are lower in intensity at small doses but grow faster than the lower-temperature components as the dose increases.

In a separate category is sample 1 g, which presented glow curves shapes that varied widely for the two different doses. The presence of a peak at about 188 °C for the 10 Gy dose suggests a radiation induced defect which only occurred for doses above 5 Gy. Although in comparison with others, this sample had the highest TL output. However, its completely distinct glow curves at these two doses suggest its anomalous behaviour in this range. The glow curve generated for the 5 Gy dose could also be due to the blackbody radiation in the reader (Balogun et al., 1999).

Summarily, for all the measurements at the considered heating rate, it was observed that samples c, d, i, k, l and m had increased peak intensity with excitation dose. As dose increases for these samples, the luminescent centre increases, leading to increased peak intensity. This means higher exposure to ionising radiation resulting to a higher number of negative and positive charges trapped. Therefore the TL intensity peak increases with an increasing gamma radiation dose. Clearly, this is a major factor to consider because for a good phosphor, intensity must increase with excitation dose. Several non-radiative recombination mechanisms could be responsible for the reduction in TL intensity with increasing dose (Kore et al., 2014) for the remaining samples within the dose range considered. These are usually associated with the defects in the crystals or levels in the middle of the band gap (deep levels) introduced by impurities – the inhibitors (McKeever, 1985; Murthy and Virk, 2013). The impurities are the atoms of the different elements present in each sample. The observed variation of the TL intensity with the excitation dose will require a more detailed experiment on defect studies (Ogundare et al., 2005).

3.2. Comparison of glow curves: similarity in mineral contents

While studying the TL glow curves of muscovites sourced from Ilesha and Ijero-Ekiti areas, Ige et al. (2006) reported that the glow peaks were only obtained after the samples have been irradiated with doses ⩾750 Gy and with a heating rate of 8 °C/s for the readouts. The TL glow curves for 8.5 kGy dose showed a single peak at 238 °C for Ijero-Ekiti samples, while
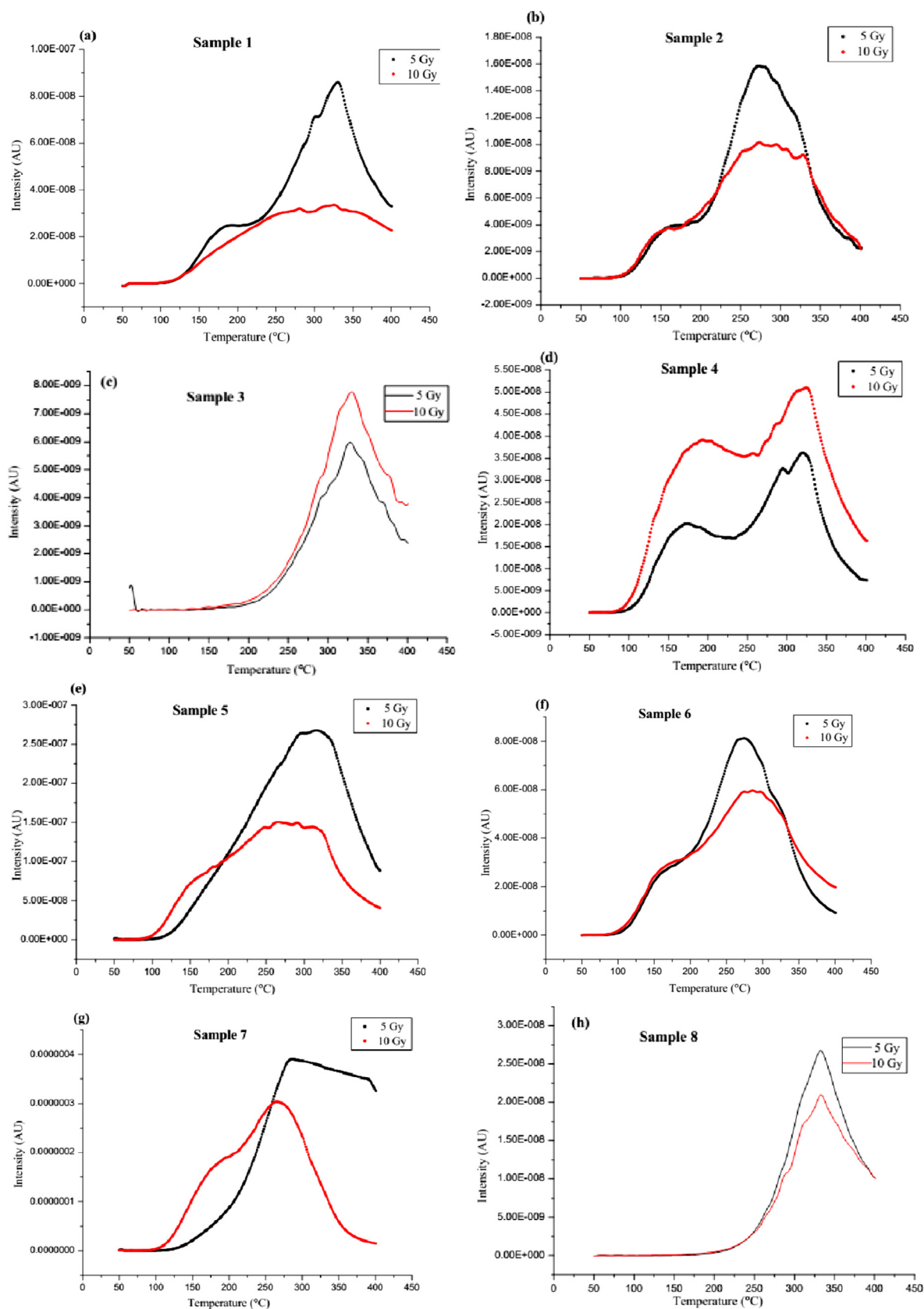
Fig. 1 (a–m) The glow curves of the samples for 5 and 10 Gy doses and at 15 °C/s heating rate.
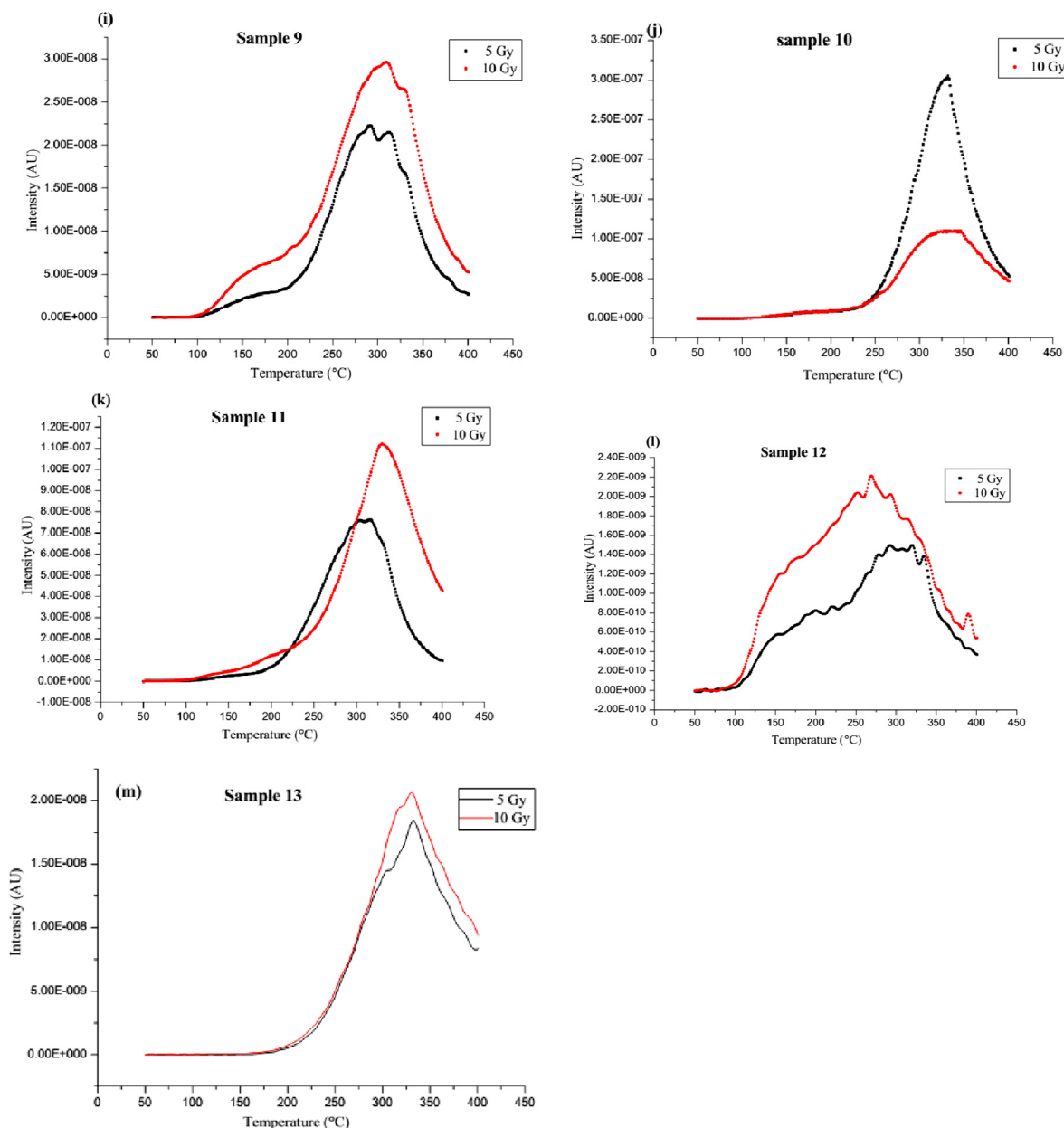
Fig. 1 (*continued*)

the Ilesha samples showed a two-peak glow curve with centroids at 238 and 330 °C (Fig. 2a). In this study, however, the glow peaks were obtained for the doses of 5 and 10 Gy but at the heating rates $\geqslant 15$ °C/s. Considering the similarity in samples from the studies, location and the TL reader, it means lower irradiation doses are capable of giving rise to glow peaks at certain heating rates. Similar to those of the earlier study, each of the samples c, h, k and m presented a distinct peak at higher temperatures (about 329, 333, 327 and 331 °C, respectively). As expected, the shifts in peak temperatures are reflecting the higher heating rate (15 °C/s) used in this study. In addition, the observed TL output in this work is higher than the one earlier reported (Ige et al., 2006). This may also be due to the possible differences in the kind and concentrations of the impurity contents of the samples.

Okumura et al. (2006) had examined the cathodoluminescence and thermoluminescence of clay minerals sourced from Clay Science Society of Japan. The clay minerals showed no noticeable glow peak in natural TL measurements with the exception of sepiolite, which produced two TL glow peaks around 210 and 260 °C (Fig. 3). The non-noticeable glow curve observed for other minerals could be as a result of the low heating rate (0.5 °C/s) used. The shape of the glow curve is similar to those presented in this present study except for samples c, h, j, k and m with each presenting at least two glow peaks at relatively high temperature ranges. Okumura et al. (2006) further stressed that, due to the non-noticeable emissions, it would be difficult to apply the clay minerals, except sepiolite, to dating for geological use.
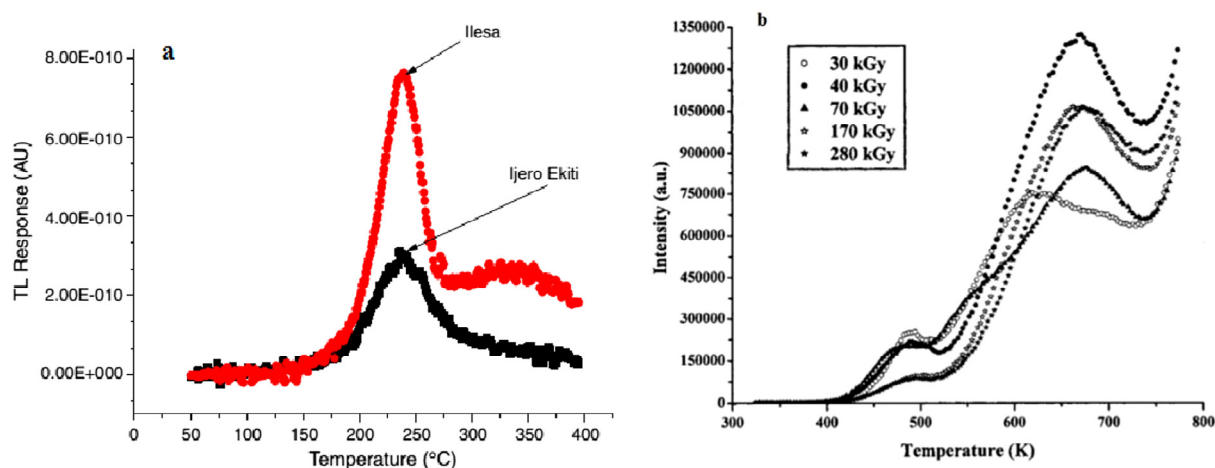
Fig. 2 (a) Glow curves of the Ilesha and Ijero-Ekiti sourced muscovites exposed to 8.5 kGy measured at 8 °C/s (Ige et al., 2006), (b) Glow curves of muscovite mica irradiated with gamma radiation of different doses (Singh et al., 2012).
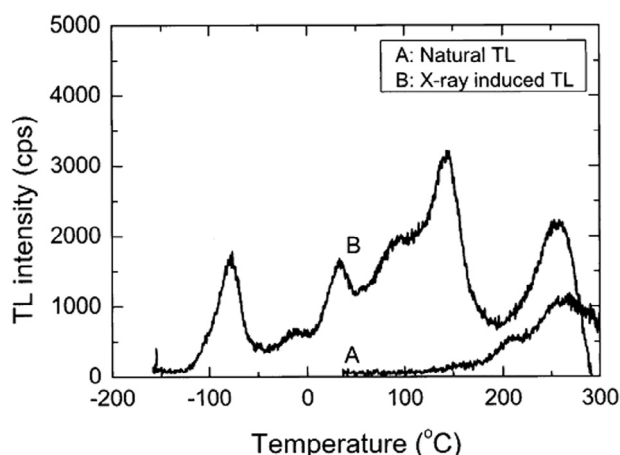

Fig. 3 TL glow curves of Sepiolite from Kuzu, Tochigi Prefecture, Japan (Okumura et al., 2006).

Thermoluminescence characteristics of high gamma dose (30–280 kGy) irradiated muscovite mica have been studied (Fig. 2b). Two prominent TL glow peaks in the temperature ranges of 218–229 °C and 347–405 °C were observed (Singh et al., 2012; Kalita and Wary, 2015). The reported glow curves are similar in shape to those of the samples a, b, d, e, f, g and i considered in this study. The two main glow peak temperatures in these samples range from 160 to 200 °C and 267 to 340 °C. This is an indication that these clay samples are essentially rich in muscovite. The glow curves of these samples are also similar to those obtained by Abdel-Razek, (2016). The author in a thermoluminescence dosimetry study using natural calcite sourced from El Bakriya, Egypt and at a heating rate of 1 °C/s, observed two high temperature peaks appearing at 283 and 359 °C in the natural glow curve (Fig. 4). The curve however has slight variations in their peak temperatures. Samples with such characteristics would be good candidates for applications in industrial gamma dosimeters especially for chemical technology and food processing related applications (Abdel-Razek, 2016). This would also lead to having inexpensive and disposable TL devices.

3.3. TL intensity with heating rate

For samples a, c, f, g, j, and k, the observed variation of peak intensity with the heating rate is quite complicated. A more detailed experimental defect studies would be required to better explain the variations. Ogundare et al., (2005) observed similar non-systematic variation while studying the heating rate effects on the thermoluminescence of fluorite. The authors reported cluster formation and thermal quenching effect as the reasons for the variations. The formation of trap clusters instead of randomly distributed defects may lead to change in the kinetics of trapping and the recombination processes, thereby influencing the TL properties of a phosphor (Mandowski and Swiatek, 1997; Ogundare et al., 2005). The effects of the heating rates on the peak intensity, the observed glow-peak and the normalised peak intensity are presented in Table 1.

From Table 1, we observed that the peak temperature increased with the heating rate for all the samples considered, except samples h and l. For sample l, although the TL intensity increased with increasing heating rate, its peak temperature shifted irregularly. The peak with the maximum intensity changes with the heating rate. The shift of the glow-peak temperature, T_m to higher temperatures as the heating rate increases is convincing. At a low heating rate, β_1, the time spent by the phosphor at a temperature, T_1 is long enough to allow the thermal release of electrons, depending on the half-life at this temperature (Kitis et al., 1993). As the heating rate increases to $\beta_2 > \beta_1$, the time spent at the same temperature, T_1 decreases. Hence the thermal release of electrons also decreases. So, a higher temperature, T_2 is needed for the same amount of thermal release to take place at β_2. Therefore, the whole glow-peak is shifted to higher temperatures as the heating rate increases in a manner that depends on the half-life and time spent at each temperature regime (Kitis et al., 1993).

On the other hand, the time lag between the formation of the peak trap and the thermal release of the trapped species could possibly be responsible for the reduction in TL intensity observed for samples a, c, f, g, j and k. The reduction in TL has been observed to have no relation with the behaviour of some particular impurity in many different materials (Kitis et al.,
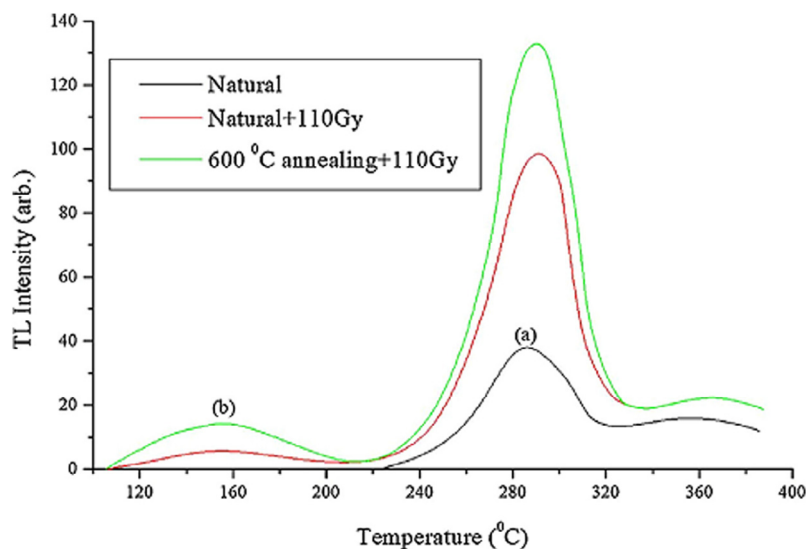
Fig. 4   TL glow curve of the calcite sample from El Bakriya. (a) Natural glow curve, (b) the natural sample following irradiation with 110 Gy and (c) the natural sample following annealing at 600 °C and irradiation with 110 Gy (Abdel-Razek, 2016).

1993). Also, as at the time of this experiment, the background under each glow peak was not zero, but rather subtracted from the glow curve of the first readout. Thus, the thermal release of the trapping specie was incomplete. So the reduction in intensity could also be due to this as well as the reasons originated in the recombination process.

To study the effect of thermal quenching, the TL intensities were normalised. That is, each T_m was divided by its respective heating rate. Since saturation of the peak is ruled out at these heating rates (due to the uniformity of dose), the decrease in the normalised TL intensity is due to thermal quenching of the luminescence centres (Yousif et al., 2015) as well as the possibility of peak saturation at doses higher than 5 Gy. However, it had been reported that a logical way to measure thermal quenching quantitatively is to record the decrease in the integrated counts (PMT current) with the increase in the heating rate at a constant dose (Kumar et al., 2010). That is, the integrated peak area (PMT current or TL- time or TL/β-temperature) must be plotted against the heating rate and the same used for the interpretation of the thermal quenching effect.

3.4. Kinetic parameters characterisation

In the calculation of the kinetic parameters, an unchanged kinetic order was assumed. The application of the variable heating rate (VHR) method for the calculation of E, involving only the T_m gives straight lines and therefore, the E values (Kitis et al., 1993). We also assumed that each glow curve comprised only single peaks at T_m. The values of E varied from 0.29 to 0.84 eV, while the S values varied from 3.7×10^1 to 4.0×10^6 s^{-1}.

As presented in Table 2, the energy traps with a higher value of activation energy suggest that fading will be lesser for such traps and as such present better prospects in dosimetry applications. Ogundare and Chithambo, (2006) had earlier evaluated the kinetic parameters of traps in thermoluminescence phosphors using the VHR method. The authors reported

Table 2   The obtained activation energy (E) and frequency factors (S) using VHR method.

Sample number	E (eV)	S (s^{-1})
A	0.72	3.9×10^5
B	0.34	1.8×10^2
C	0.52	5.9×10^3
D	0.29	3.7×10
F	0.43	1.5×10^3
G	0.48	9.4×10^3
I	0.32	8.7×10
J	0.79	1.7×10^6
K	0.51	4.7×10^3
M	0.84	4.0×10^6

the E for peaks with temperature around 198 and 293 °C to be 1.43 and 1.62 eV while it was 1.1×10^{14} and 1.2×10^{13} s^{-1} for S. Also, Ogundare et al. (2006c) calculated the activation energy of muscovite samples sourced from Ijero-Ekiti, using the three point technique and first order deconvolution function (Kitis et al., 1998). The authors reported E values of 0.835 ± 0.101 and 0.830 eV while the S values were calculated to be 1.01×10^7 and 4.56×10^7 s^{-1}. The reported values are higher than those in this work except for sample m with nearly equal values for these parameters. We noted, as expected, the wide departure of these values from those in the literature depicting the non-representation of the process by the assumed conditions as well as the differences in the experimental procedures. However, reliable results have been obtained, especially in the case of samples j, k and m whose single peaks were observed, the heating rate used notwithstanding.

The trapping parameters like the frequency factor, S and the kinetic order, b can be influenced by the heating rate (Kitis et al., 1993). Furthermore, the frequency factor is temperature dependent (Chen and Kirsh, 1981) and the order of

kinetic varies during the readout. Therefore, the values presented in Table 2 are an approximation of the trap depth, E and the frequency factor, S (Azorin et al., 1985). A heating protocol would be necessary to isolate each peak for the calculation of their kinetic parameters.

4. Conclusions

The thermoluminescence characteristics of clay samples from certain mineral rich environments have been studied. The glow curves of some samples at 5 and 10 Gy doses showed that they are essentially muscovite in nature. While samples a, b, d, e, f, g and i presented two prominent peaks at about 160–200 °C and 267–340 °C, a high-temperature peak was observed for samples c, h, k and m at about 329, 333, 327 and 331 °C, respectively. Furthermore, samples c, d, i, k, l and m showed increased peak intensity with increasing excitation doses. These glow peaks were noted to be a complex trapping system, consisting of several overlapping first order glow peaks and each with a different thermoluminescent behaviour except for samples c and m that showed independence of peak temperature with excitation dose.

We noted that as the heating rate increases, the peak temperature of the glow-peaks shifted to higher temperatures for all the samples, except h and l, in agreement with the dynamic nature of the heating rate in influencing the glow peaks characteristics. We also observed that samples b, d, e, h, i, l and m exhibited increase in peak height with the heating rate and faster registration of the glow curves, a requirement for thermoluminescence dosimetry in large-scale personnel monitoring. The obtained activation energies, E and frequency factors, S are lower when compared with earlier reported values, especially for similar samples except sample m with comparable data. The lower values have been attributed to the variation in the experimental procedure and difference in samples.

In all, samples c, d, i, k and m were considered the most suitable for thermoluminescence applications since they exhibited increased peak intensity with increasing excitation dose, which is the basis for thermoluminescence dosimetry. These samples would be invaluable in industrial related gamma dosimetry applications and the reduction in thermoluminescence intensity must be considered for high heating rates applications.

References

Abdel-Razek, Y.A., 2016. Thermoluminescence dosimetry using natural calcite. J. Taibah Univ. Sci. 10, 286–295.

Akinola, O.O., Oluwatoyin, O., Ademilua, O.L., Oladimeji, L., 2014. Compositional features and functional industrial applications of the lateritic clay deposits in Oye-Ekiti and Environs, Southwestern Nigeria. Int. J. Sci. Technol. 2 (9), 6–12.

Aramide, F.O., Alaneme, K.K., Olubamba, P.A., Borode, J.O., 2014. Characterization of some clay deposits in South West Nigeria. Leonardo Electron. J. Pract. Technol. 25, 46–57.

Azorin, J., Gutierrez, A., Martinez, C.G., 1985. Determination of activation energies and frequency factors of CaSO4: Dy thermoluminescent dosimeters. Radiat. Effects 84, 263–280.

Balogun, F.A., Ojo, J.O., Ogundare, F.O., Fasasi, M.K., Hussein, L.A., 1999. TL response of a natural fluorite. Radiat. Meas. 30, 759–763.

Chen, R., Kirsh, Y., 1981. Analysis of Thermally Stimulated Processes. Pergamon Press, Oxford.

Egbe, N.O., Heaton, B., McCallum, S., 2010. Clay as thermoluminescent dosemeter in diagnostic radiology applications. Nigerian J. Med. 19 (2), 177–183.

Fasasi, A.Y., Balogun, F.A., Fasasi, M.K., Ogunleye, P.O., Mokobia, C.E., Inyang, E.P., 2007. Thermoluminescence properties of barium titanate prepared by solid-state reaction. Sens., Activators A 135, 598–604.

Gökçe, M., Oğuz, K.F., Karalı, T., Prokic, M., 2009. Influence of heating rate on thermoluminescence of Mg₂SiO₄: Tb dosimeter. J. Phys. D Appl. Phys. 42 (10). http://dx.doi.org/10.1088/0022-3727/42/10/105412.

Hoogenstraaten, W., 1958. Electron traps in zinc-sulphide phosphors: Philips. Res. Rep. 13, 515–693.

Ige, O.A., Tubosun, I.A., Ogundare, F.O., Mokobia, C.E., Balogun, F.A., 2006. TL response of muscovite samples from granite pegmatite of Ilesa and Ijero-Ekiti, Southwestern Nigeria. Radiat. Meas. 41, 967–970.

Iyang, E.P., Taleatu, B.A., Oketayo, O.O., Mokobia, C.E., Adenodi, R.A., Balogun, F.A., 2011. Characterizing thermoluminescence properties of calcium halophosphate fluorescent coating powder for radiation dosimetry. J. Environ. Sci. Eng. 53 (1), 1–6.

Kalita, J.M., Wary, G., 2015. Dosimetric characteristics of muscovite mineral studied under different annealing conditions. Phys. Scr. 90 (5), 55702–55707.

Kaur, N., Singh, M., Singh, L., Lochab, S.P., 2013. Investigation of thermoluminescence characteristics of gamma irradiated phlogopite mica. Radiat. Phys. Chem. 87, 26–30.

Kirsh, Y., 1992. Kinetic analysis of thermoluminescence. Phys. Status Solidi A 129, 15–48.

Kitis, G., Spiropolu, M., Papadopoulos, J., Charalambous, S., 1993. Heating rate effects on the TL glow-peaks of three thermoluminescent phosphors. Nucl. Instrum. Methods Phys. Res. 73, 367–372.

Kitis, G., Gomez-Ros, J.M., Tuyn, J.W.N., 1998. Thermoluminescence glow-curve deconvolution functions for first, second and general orders of kinetics. J. Phys. D 31, 2636–2641.

Kore, B.P., Dhoble, N.S., Dhoble, S.J., 2014. Synthesis and thermoluminescence characterization of Na₆Mg(SO₄)₄:RE (RE = Ce, Tb) phosphors. Radiat. Meas. 67, 35–46.

Kumar, M., Chourasiya, G., Bhatt, B.C., Sunta, C.M., 2010. Dependence of peak height of glow curves on heating rate in thermoluminescence. J. Lumin. 130, 1216–1220.

Malomo, S., 2011. Framework for and opportunities for sustainable private sector participation in solid minerals development in Ekiti State. In: Ekiti State Economic Development Summit. Proceedings of Nigerian Geological Survey Agency.

Mandowski, A., Swiatek, J., 1997. Trapping and recombination properties due to trap clustering. J. Phys. III France 7, 2275–2280.

McKeever, S.W.S., 1985. Thermoluminescence of Solids. Cambridge University Press, Cambridge.

Mokobia, C.E., 2010. Investigating the dosimetric potentials of natural marble. J. Phys. Sci. Innov. 2, 18–25.

Mokobia, C.E., 2012. A study of the thermoluminescence fading characteristics of natural marble phosphor. Sci. Afr. 11 (2), 35–40.

Murthy, K.V.R., Virk, H.S., 2013. Luminescence phenomena: an introduction. Defect Diffusion Forum 347, 1–34.

Ogundare, F.O., Chithambo, M.L., 2006. Accuracy of the activation energy calculated from a thermoluminescence glow-peak using a method that uses three points on the peak. Phys. Status Solidi A 3 (2), 355–361.

Ogundare, F.O., Chithambo, M.L., 2007. Thermoluminescence kinetic analysis of quartz with a glow peak that shifts in an unusual manner with irradiation dose. J. Phys. D Appl. Phys. 40, 247–253.

Ogundare, F.O., Balogun, F.A., Hussain, L.A., 2004. Kinetic characterization of the thermoluminescence of natural fluorite. Radiat. Meas. 38, 281–286.

Ogundare, F.O., Balogun, F.A., Hussain, L.A., 2005. Heating rate effects on the thermoluminescence of natural fluorite. Radiat. Meas. 40, 60–64.

Ogundare, F.O., Balogun, F.A., Olowofela, J.A., Mokobia, C.E., Fasunwon, O.O., 2006a. Thermoluminescence characteristics of natural dolerite. Nucl. Instrum. Methods Phys. Res. B 243, 156–160.

Ogundare, F.O., Chithambo, M.L., Oniya, E.O., 2006b. Anomalous behaviour of thermoluminescence from quartz: a case of glow peaks from a Nigerian quartz. Radiat. Meas. 41, 549–553.

Ogundare, F.O., Balogun, F.A., Hussain, L.A., 2006c. Evaluation of kinetic parameters of traps in thermoluminescence phosphors. Radiat. Meas. 41, 892–896.

Okumura, T., Nishido, H., Ninagawa, K., Sakamoto, T., 2006. Cathodoluminescence and thermoluminescence studies of clay minerals. Clay Sci. 13, 59–68.

Okunola, O., Egbulem, C., 2015. Geological setting, compositional and economic appraisal of clay-shale occurrence in Itu-Mbonuso/Iwere Area, South-Eastern Nigeria. J. Geogr. Geol. 7 (1), 85–96.

OlaOlorun, O., Oyinloye, A., 2010. Geology and geotechnical appraisal of some clay deposits around Ijero-Ekiti Southwestern Nigeria: implication for industrial uses. Pak. J. Sci. Ind. Res. 53 (3), 127–135.

Olise, F.S., Akinnagbe, D.M., Olasogba, O.S., 2016. Radionuclides and radon levels in soil and ground water from solid minerals-hosted area, South-western Nigeria. Cogent Environ. Sci. 2, 1142344. http://dx.doi.org/10.1080/23311843.2016.1142344.

Ologe, O., Ogungbemi, O.S., Alu, O.O., 2014. Mining activities and its hydrogeochemical implication: a case study of Ijero Mining Site Southwestern Nigeria. Pac. J. Sci. Technol. 15 (2), 298–308.

Oyinloye, A.O., Adebayo, O.F., 2005. Petrophysical and chemical properties of calc-gneiss and clay deposit in Ijero-Ekiti area as industrial raw materials. Global J. Mech. Eng. 6, 30–34.

Singh, L., Kaur, N., Singh, M., 2012. Thermoluminescence characteristics of high gamma dose irradiated muscovite mica. Indian J. Pure Appl. Phys. 50, 14–18.

Woda, C., Schilles, T., Rieser, U., Mangini, A., Wagner, G.A., 2002. Point defects and the blue emission in fired quartz at high doses: a comparative luminescence and EPR study. Radiat. Prot. Dosimetry. 100, 261–264.

Yazici, A.N., Chen, R., Solak, S., Yegingil, Z., 2002. The analysis of thermoluminescent glow peaks of CaF2: Dy (TLD-200) after β-irradiation. J. Phys. D Appl. Phys. 35 (20), 2526–2535.

Yousif, A., Som, S., Swart, H.C., 2015. Photoluminescence and thermoluminescence properties of Y3(Al, Ga)$_5$O$_{12}$:Tb3+ Phosphor. J. Mod. Opt. 63 (2), 103–110.